# Role of riparian wetlands and hydrological connectivity in the dynamics of stream thermal regimes

Jonathan J. Dick, Doerthe Tetzlaff and Chris Soulsby


## ABSTRACT

Stream temperature is a fundamental physical characteristic of rivers, influencing biological productivity and water quality. Given the implications of climate warming for stream thermal regimes, it is an important consideration in river management plans. Energy exchanges at the water–air interface, channel geomorphology, riparian vegetation and advective heat transport from the different sources of discharge can all influence stream temperature. A simple mixing equation was used to investigate heat transport and to estimate daily mean and maximum stream temperatures on the basis of mixing groundwater and near-surface flows from riparian wetlands as end-members in a peatland catchment. The resulting data were evaluated against energy balance components and saturation extent to investigate the importance of riparian wetlands in determining stream temperatures. Data fit was generally good in periods with extensive saturation and poorest in dry periods with less hydrological connectivity, when reduced saturation and low flows increased the relative influence of energy exchange at the stream–atmosphere interface. These findings have implications in terms of climate change and land management, where the planting of riparian buffer strips to moderate water temperatures may be less effective when saturation area is extensive and hydrological connectivity is high.


**Key words** | mixing models, peatlands, riparian areas, stream temperatures

**Jonathan J. Dick** (corresponding author)
**Doerthe Tetzlaff**
**Chris Soulsby**
School of Geosciences,
University of Aberdeen,
Elphinstone Road, Aberdeen AB24 3UF,
UK
E-mail: *j.j.dick@ljmu.ac.uk*

**Jonathan J. Dick**
School of Natural Sciences and Psychology,
Liverpool John Moores University,
Liverpool,
UK

**Doerthe Tetzlaff**
IGB Leibniz Institute of Freshwater Ecology and Inland Fisheries,
Berlin,
Germany
and
Humboldt University Berlin,
Berlin,
Germany

## INTRODUCTION

Stream temperature is a critical riverine water quality characteristic, strongly influencing biogeochemistry, ecological productivity and species distribution (Isaak & Hubert 2001; Malcolm *et al.* 2004; Caissie 2006). It is principally controlled by hydroclimatic factors (e.g., net radiation fluxes at the atmosphere–stream interface) and modulated by landscape characteristics (Caissie 2006). Landscape effects on stream temperatures have been a research focus, including the effects of shading (by riparian vegetation and topography), elevation and channel morphology (Mosley 1983; Imholt *et al.* 2013). Recent work has also considered coupled heat transfers in groundwater (GW)–surface water systems to assess how spatio-temporal dynamics in the magnitude, connectivity and thermal properties of various runoff sources affect stream temperatures (Kurylyk *et al.* 2014).

Interests in energy exchange and heat transfer have focused on riparian areas where energy exchange processes have greatest potential to affect stream temperature (Garner *et al.* 2015). These include vegetation shading (Brown *et al.* 2010), GW inflows (Constantz 1998) and hyporheic exchange (Birkel *et al.* 2016). An important part of many headwaters are wetland-dominated riparian areas where GW discharge is strong and the water table is close to the ground surface (Ingram 1983; Geris *et al.* 2014). High GW tables create areas of dynamic saturation that can expand and contract,

doi: 10.2166/nh.2017.066

depending on antecedent hydrometeorological conditions (Dunne *et al.* 1975; Birkel *et al.* 2010). The spatial extent and connectivity of such riparian wetlands determine the water sources generating stream flow and the relative importance of near-surface flow (NSF) paths and GW inflows (Dick *et al.* 2014; Tetzlaff *et al.* 2014). Under wet conditions, riparian wetlands are strongly connected to the stream network and the saturation zone may expand to upslope areas (Blumstock *et al.* 2015). Such saturation zones form extensive areas for atmosphere–water energy exchange, away from the channel network, affecting the thermal characteristics of such runoff sources (Dick *et al.* 2014). In extensive riparian wetlands, up to 80% of annual streamflow can be generated from NSF paths (Tetzlaff *et al.* 2014), which may have a significant influence on stream temperatures (Dick *et al.* 2015). Given the spatial extent and downstream influence of low order streams, the implications may extend beyond headwaters (Bishop *et al.* 2008). To date, there has been limited work on the importance of such saturated areas in catchment thermoscapes.

This research gap has implications for river management decisions. Recent interest has centred on riparian areas, where management has focused on creation of buffer strips, to improve freshwater quality and the aquatic environment (Osborne & Kovacic 1993). The ability to focus riparian management on specific areas as 'hot spots' represents its main attraction, given it is likely to yield the best cost–benefit ratios (Hrachowitz *et al.* 2010). Riparian areas have been the focus for re-forestation as resilience-building measures to mitigate climate change which is projected to lead to an increase in temperatures of over 2°C in eastern Scotland by 2080 under low emission scenarios (Murphy *et al.* 2009) and has potential to increase stream temperatures (Zwieniecki & Newton 1999; Broadmeadow *et al.* 2011). Usually, financial constraints of such schemes dictate that bankside planting is limited to areas immediately fringing streams to maximise the shading effect (Johnson & Wilby 2015). However, this approach may have limitations in environments where riparian wetlands result in prolonged and spatially extensive saturation for water–atmosphere energy exchanges to cross (Kuglerová *et al.* 2014). In such cases, a broader view of catchment thermoscapes may be needed to understand the dynamics of surface saturation and its effect on heat transfer to streams.

In this work, we focus on a peatland-dominated catchment in the Scottish Highlands. Previous work has shown that the peatland is the main hydrological source area contributing to the dynamics of stream flow generation (Soulsby *et al.* 2015). Also, data have been collected on the catchment thermoscapes in the stream and various source waters to assess the wider catchment controls on stream temperatures (Dick *et al.* 2014). Here, we use a simple mixing model to assess the importance of well-connected riparian wetlands for stream temperatures. Such mixing models have been useful for investigating the role of changing water sources in catchments and have been widely applied in hydrograph separations (e.g., Buttle 1994; McNamara *et al.* 1997) typically involving the mixing of assumed conservative solutes to quantify contributing sources waters (e.g., Ockenden *et al.* 2014). Earlier work utilised contrasting thermal characteristics of different source waters as a tracer in mixing equations (Shanley & Peters 1988); and similar approaches have been used to identify point source inputs of GW along streams (Selker *et al.* 2006).

The specific objectives were to:

1. predict mean and maximum daily stream temperatures using a simple two-component mixing model to assess the extent to which the fluxes and thermal properties of NSF and GW can explain stream water temperatures;
2. ascertain how temporal variations in riparian wetland extent and hydrological connectivity influence the stream thermal regime;
3. address the implications of these findings for riparian management strategies used to curb the effects of climate change on stream temperatures.

## STUDY SITE

The Bruntland Burn (Figure 1) is a 3.2 km$^2$ catchment in the Scottish Highlands, described in detail by, for example, Tetzlaff *et al.* (2007) and Birkel *et al.* (2011). The catchment is of glacial origin with a wide flat valley bottom receiving drainage from steeper hillslopes. Elevation spans 248 to 539 m.a.s.l., with mean slopes of 13°. Land cover is mostly heather (*Calluna vulgaris* and *Erica tetralix*) moorland on steeper slopes, with limited forest cover. The only significant

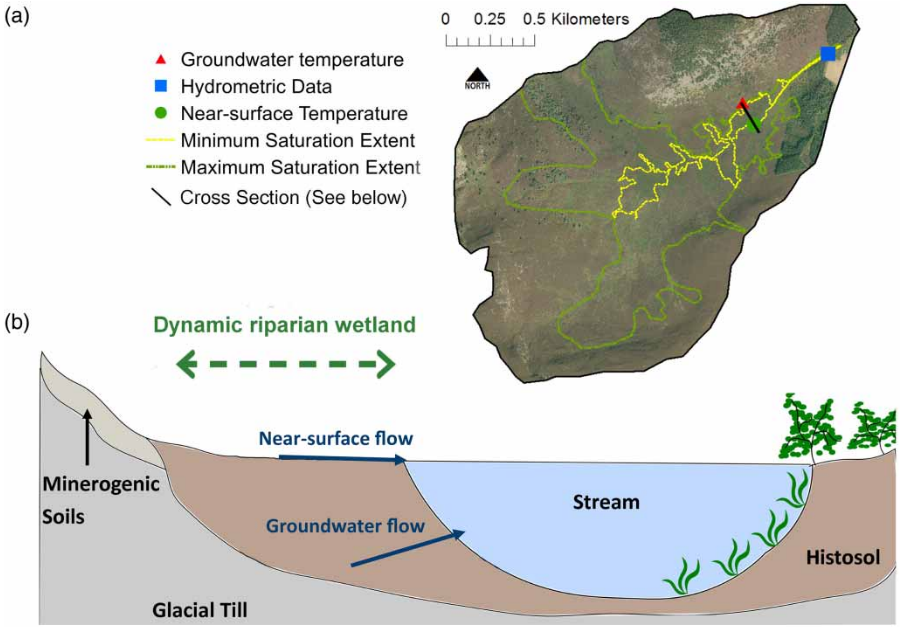


**Figure 1** | Study site (a) showing minimum and maximum spatial extents of the saturated riparian wetland along with measurement locations. The transect line on the map corresponds to schematic cross section (b) through the dynamic riparian wetlands showing components of water and temperature fluxes.

riparian tree shading is at the catchment outlet, where a plantation fringes the south of the stream, although the channel dimensions coupled with shrub growth can give local areas of shading (Dick *et al.* 2014). Riparian areas cover ~10% of the catchment and are characterised by *Sphagnum* spp. and purple moor-grass (*Molinia caerulea*) on 1–2 m deep peats (histosols).

Mean annual precipitation is ~1,000 mm, mostly from low intensity frontal events. Mean annual runoff is 700 mm and potential evapotranspiration is 400 mm per year. Mean annual air temperature is ~6°C, with daily means ranging between 12°C and 1°C in July and January, respectively (Dick *et al.* 2015).

A dominant feature of the hydrology of the catchment are extensive riparian saturation zones that dynamically expand and contract in response to precipitation (Figure 1). The saturated area covers 2–60% of the catchment, depending on antecedent conditions (Birkel *et al.* 2010). Most precipitation events instigate a streamflow response, as water is displaced from these riparian zones as saturation-excess overland flow (Birkel *et al.* 2010) which contributes around 80% of annual streamflow (Soulsby *et al.* 2015). Runoff coefficients are typically <10%, increasing in wetter periods to >40% as the saturated zone in the riparian wetland expands (Tunaley *et al.* 2016), and connects lateral flow in the upper horizons of the hillslope podzols to the channel network (Tetzlaff *et al.* 2014). Shallow (<0.5 m) peats cover the lower hillslopes (~22% of the area). Steeper slopes are covered by podzols with a 0.1–0.2 m deep O horizon overlying free-draining mineral sub-soil, which facilitates deeper GW recharge. Direct GW inputs to the stream account for 20% of annual runoff (Ala-aho *et al.* 2017).

The stream channel is narrow (0.5–1 m) and deep (0.5–1.5 m), with a limited hyporheic zone, due to being lined by peat or the underlying glacial drift (Figure 1). Point source influxes of surface waters draining from the adjacent riparian wetlands are located throughout the stream network.

Dick *et al.* (2015) measured stream temperature at 11 locations throughout the catchment, and GW and surface water (each at 4 locations). Their measurements showed little spatial variability in stream water temperature, which exhibited an annual average of 6.3°C (range of 18.2°C). The dynamic riparian wetland NSF temperatures showed most variability, with an average temperature of 6.4°C and range of 23.8°C (Dick *et al.* 2015). The deeper GW had the least variable temperature with a range of 3.2°C and an average of 7.0°C. Shallower GW fell between the NSF and deeper GW, and its temperature range decreased with depth (Dick *et al.* 2015).

## DATA AND METHODS

Hydrometric monitoring covered approximately two years between 1 July 2012 and 30 September 2014. Seasons were defined meteorologically (summer starting 1 June; autumn 1 September; winter 1 December; spring 1 March). An automatic weather station 2 km away measured precipitation (Campbell ARG100 tipping bucket rain gauge; error of 0.05 mm), air temperatures (Campbell HMP35AC probe; error of 0.2°C), radiation (NR Lite net radiometer; error of 5%), humidity (Campbell HMP35AC probe; error of 1–3%) and wind speed (Vector A100R anemometer; error of 0.25 m $s^{-1}$) (Hannah *et al.* 2004). We used relative air pressure from the Met Office weather station at Braemar (c. 30 km away) to estimate the energy balance components of latent and sensible heat. Discharge was estimated at the catchment outlet (Hydrometric data – Figure 1) at 15 minute intervals using a rating equation in a stable section with stream stage height measured with a water level recorder (Odyssey data recording loggers; resolution of around 0.8 mm).

GW, NSF and Q water temperatures were measured using TinyTag TGP-4017 loggers (Gemini data loggers; precision of 0.5°C) (Figure 1). Due to logistical and storage constraints, a 1 hour recording interval was used, accounting for thermistor response time (25 minutes), and download frequency. Loggers were laboratory calibrated across a greater than natural temperature range before and after installation, maintaining 0.5°C accuracy. Stream temperature was measured on the bed, with loggers enclosed in white shields, reducing effects of incident radiation. NSF temperature was measured on the surface of the dynamic riparian wetland in the riparian zone, again within radiation shields. GW temperature was measured in a borehole, situated in a spring on the north side of the catchment (Figure 1).

### Modelling and analysis

A two-component mixing equation (Kendall & McDonnell 1998) was used to explore the extent to which stream temperature variations could be explained by mixing NSF and GW inputs to the stream. We hypothesised that the ability to estimate stream temperature would relate to wetness (i.e., saturation area extent) and atmospheric energy inputs. Daily mean and maximum stream water temperatures $T_S$ were predicted using the water temperature, discharge ($Q_S$), and flux end-members representing NSF ($Q_{NSF}T_{NSF}$) and GW ($Q_{GW}T_{GW}$).

$$T_S = \frac{Q_{NSF}T_{NSF} + Q_{GW}T_{GW}}{Q_S} \quad (1)$$

For the temperatures of each flux ($T_{NSF}$ and $T_{GW}$), daily means (or daily maximum) of the NSF and GW temperature measurements were used. The sensors chosen to represent the end member were selected based on previous analysis (Dick *et al.* 2015), which showed the loggers to be representative of the end members as defined by this study. They were specifically chosen as the NSF was highly variable and the GW low variability. The non-parametric Wilcoxon signed rank test was used to assess the temperature difference between stream loggers, and showed no significant difference ($p$-value = 0.97). Therefore, measurements from the logger at the outlet were used for $T_S$. The NSF observation site was specifically chosen as it was the closest to the stream location where most NSF fluxes from the saturated area occur (Soulsby *et al.* 2015). The four NSF temperature loggers were not significantly different ($p$-value = 0.05) (Dick *et al.* 2015). For GW, recent work (Scheliga *et al.* 2017) has shown similarly damped thermal regimes in four deep GW wells, therefore, the GW spring shown in Figure 1 was deemed representative as an end member.

GW and NSFs water fluxes ($Q_{NSF}$ and $Q_{GW}$) were impractical to measure directly and are temporally variable; therefore, we used modelled estimates from a tracer-aided conceptual model of Soulsby *et al.* (2015). The model simulated streamflow $Q_S$, $Q_{NSF}$ and $Q_{GW}$ from conceptual storages representing the riparian saturation zone and deeper GW. It was calibrated to stream and soil water isotope data, soil moisture and GW levels (Birkel *et al.* 2015). To assess uncertainty in the modelled fluxes from each landscape unit, the 5th and 95th percentiles of the NSF and GW flux estimates from the calibrated model (from 500 retained parameter sets) were used.

Importantly, we also estimated a daily time series of the spatial extent of the saturation area in the riparian wetland, using an algorithm based on precipitation, antecedent wetness and a soil moisture parameter over the previous 7 days, described by Birkel *et al.* (2010). The procedure was calibrated against field mapping. For validation, the extent of wetness was surveyed in the field under five different sets of hydrological conditions and regressed against past hydrometeorological conditions to estimate the relationship between precipitation, discharge and evapotranspiration in the previous 7 days. Once the relationship was established, high frequency measurements of precipitation, discharge and the calculation of evapotranspiration enabled the construction of a time series. Additionally, a detailed soil survey broadly linked the minimum saturation extent to the permanently saturated deep peats, and the maximum saturation extent to the temporarily saturated gleysols. The saturation extent was a good proxy for the connected area of the catchment contributing directly to stream flow through NSFs, and was central to the analysis. This is because the extent of saturation determines the area of the catchment contributing to streamflow via NSFs, which may be up to 70% in the wettest periods (Dick *et al.* 2014; Blumstock *et al.* 2015). We also used GW levels in the riparian wetlands as a qualitative way of linking saturation extent with near-surface hydrological conductivity. The findings of Blumstock *et al.* (2015) (in a study in the same catchment) found a strong link between soil water, GW, and stream water chemistry and GW level for the same catchment.

Data were analysed for the whole period and by meteorological seasons (summer: June–August, autumn: September–November, winter: December–February, spring: March–May). However, as the period was two years and two months, summer 2012 only comprised July and August and autumn 2014 only September. Our analysis was therefore extended to include the greatest variability in hydroclimate.

To assess goodness-of-fit between measured and estimated stream temperatures, the Nash–Sutcliffe (NSE) and Kling–Gupta (KGE) efficiency statistics were used (Nash & Sutcliffe 1970; Gupta *et al.* 2009) (as they compare the mean square error to the variance) along with the root mean square error (RMSE) and coefficient of variation (CV). We also used the Spearman's rank order correlation test with the estimated daily mean and maximum stream temperature data to assess the correlation of the difference between daily measured and estimated temperatures with the saturation area extent, GW levels and energy balance components, in order to evaluate their potential influence. This analysis was conducted for the whole study period, each season, and for saturation extents less than 12% of the area.

## RESULTS

### Stream thermal regime and catchment hydrological dynamics

Air (Figure 2(b)) and stream temperatures (Figure 3(a)) followed seasonal patterns, reflecting variations in incoming radiation (Figure 2(a)). Summer 2012 had the highest June/July rainfall in NE Scotland for 100 years with 404 mm of rain which was 167% of the average (1981–2010), and below average temperatures of 12 °C, against an average of 12.2 °C (Met Office 2012). The large rainfall events caused high early summer stream fluxes, followed by low fluxes during late summer and early autumn (Figure 2(d)). Fluxes increased in mid-autumn and early winter in response to larger precipitation events. Below average temperatures then followed in late winter and spring 2013 (0.2 °C and 1.5 °C below average, respectively). These below-average

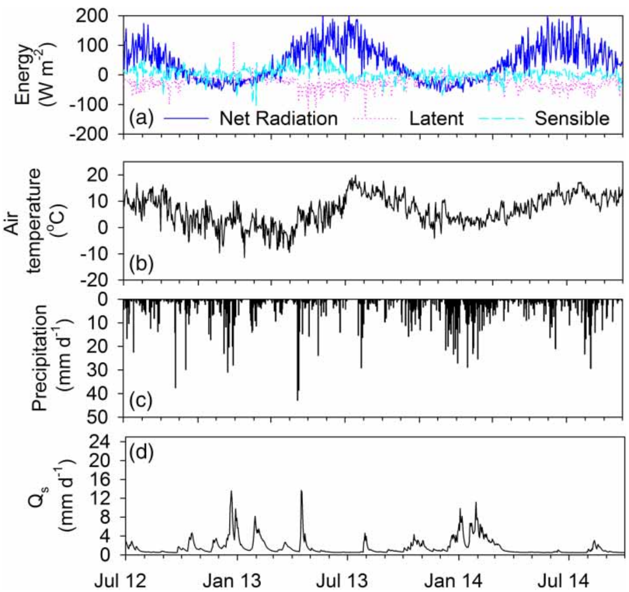


**Figure 2** | Hydrometric data: (a) radiative exchanges; (b) air temperature; (c) precipitation; (d) discharge.

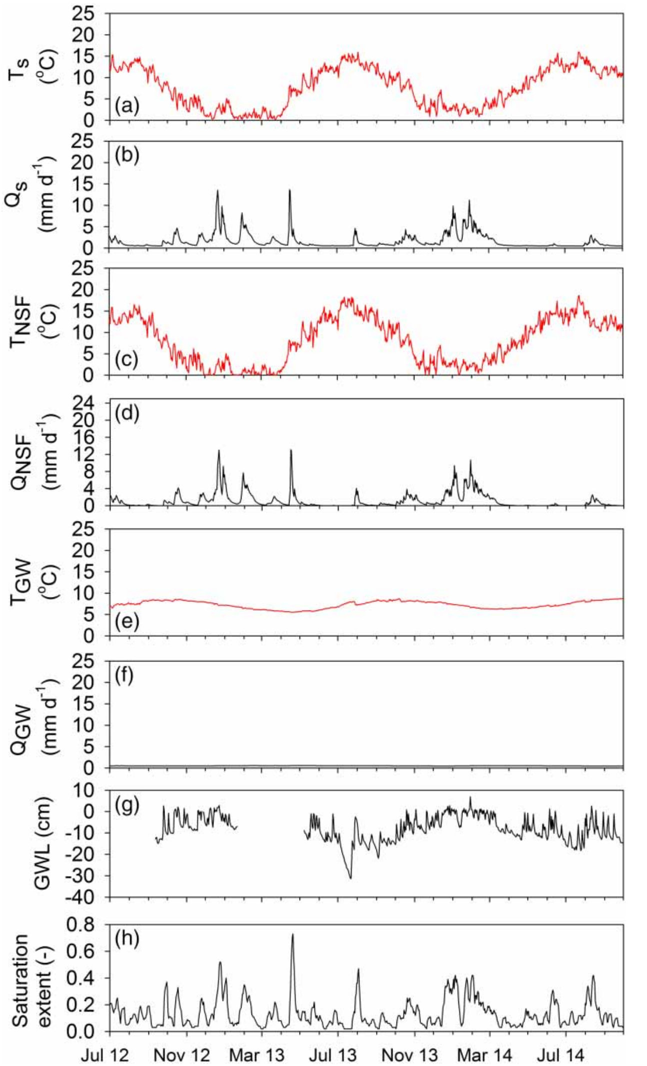


**Figure 3** | Time series graphs for the measured stream water temperature (a) and discharge (b). The lower plots show the input data for near surface component (NSF) water temperature (c) and water flux (d); and the groundwater (GW) components of temperature (e) and water flux (f). Panel (g) is the GW level in the valley bottom peat and (h) is the catchment saturation extent as fraction of the catchment.

temperatures persisted until mid-spring (Met Office 2013a, 2013b). Summer 2013 was the warmest in 10 years with average temperatures of 13.8 °C (1.1 °C higher than the average), and 183 mm of rainfall (73% of the average) (Met Office 2013c), however, it was punctuated by significant rainfall at the end of July. Drought conditions afterwards persisted until rewetting in autumn. Winter in 2013–2014 had above average rainfall of 587 mm (177% of the average), with large December–January rainfall events (10 year return period) generating increased flows (Met Office 2014). Spring 2014 followed with 227 mm of rain (93% of the average), ahead of a summer which had above-average rainfall of 301 mm (or 120% of the average).

Riparian GW levels remained high throughout the autumn, winter and spring periods (Figure 3(g)), fluctuating between ~1 and 2 cm above the surface in wettest conditions and ~20 cm below the surface when dry, although in summer 2013 they fell to ~30 cm deep. GW levels generally reflected the seasonal dynamics of the extent of the saturated area (with higher GW levels reflecting the wetter winters), although short-term rainfall events caused ~10 cm increases in water levels in response to NSF in the peat. During periods with high rainfall, saturation was estimated to have reached a spatial extent of >35% of the catchment (Figure 3(h)) (e.g., December 2012, early 2013, April/May 2013 and December 2013/January 2014). More generally, the saturation extent was <20% and >5% for the driest periods.

## Dynamics in input data and energy balance components

Figure 3 shows the time series of stream temperatures and flow (Figure 3(a) and 3(b)) in relation to measured temperatures and modelled fluxes of NSFs (Figure 3(c) and 3(d)) and GW (Figure 3(e) and 3(f)). Descriptive summary statistics are presented in Figure 4. The temperatures time series were tested using the Wilcoxon signed rank test, and were significantly different ($p = 0.05$). Stream flux response

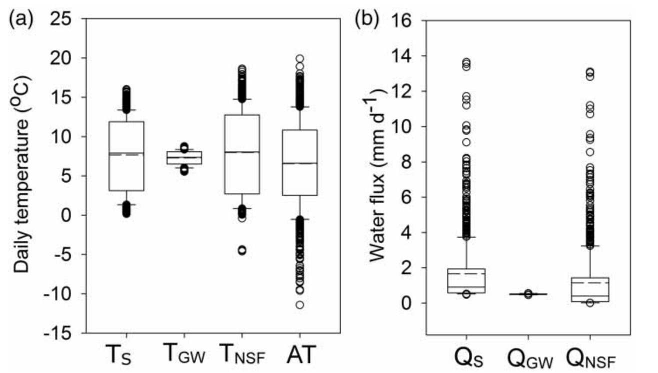


**Figure 4** | Box plots of the daily temperatures (a) and water fluxes (b). The whiskers represent the 90th and 10th percentiles, the box limits are the 75th and 25th percentiles, the solid centre line is the median and the dashed line the mean. The hollow points are the outliers.

(Figure 3(b)) was similar to modelled NSF response, reflecting the dominance of overland flow from the riparian wetland in generating storm runoff (Figure 3(d)), when the extent of the saturation zone was highest (Figure 3(h)). The driest spell in the study period was summer 2013 (Figure 3(b) and 3(d)) (Met Office 2013c), when NSFs decreased and eventually ceased, leading to decreased discharge, as the riparian wetlands disconnected from the stream network (cf. Figure 3(d) and 3(h)) (see Dick *et al.* 2014), leading to deeper GW fluxes dominating runoff generation remaining stable with low variability through the year (Figure 3(f)).

Both stream and NSF temperatures followed seasonal patterns, but also exhibited day-to-day variability reflecting prevailing hydroclimatic conditions (Figure 3(a) and 3(c)). Stream temperature was damped (showing a reduced range) when compared to NSF, reflecting moderation by more stable GW temperatures (Figure 4). In contrast, GW temperatures varied little, with a mean of 7.0°C, being ~1°C higher in summer and ~1°C lower in winter (Figure 3(e)). Previous work has shown that GW is mainly derived from glacial drift deposits which are up to 30 m deep and well mixed isotopically (Soulsby *et al.* 2016). Thus, recharge temperatures usually are preserved and moderated as different recharge sources mix (Scheliga *et al.* 2017).

Figure 2(a) shows the dynamics of different energy balance components from the Girnock weather station. Net radiation dominates with an average of: 42 W $m^{-2}$ over the study period, being an energy source in summer (with an average of 45 W $m^{-2}$), also a sink in winter when short wave is low (with an average of –21 W $m^{-2}$), given the northerly (57°) latitude. Latent heat transfers being a sink in summer (–36 W $m^{-2}$), but occasionally a source during winter (with an average of –13 W $m^{-2}$, but highs of ~20 W $m^{-2}$). Sensible heat fluctuated around 0 W $m^{-2}$.

## Measured versus estimated stream temperatures

It was evident that stream temperatures were not fully described as a simple mix of GW and NSFs in the two-component mixing equation, although many features were captured. Differences between measured and estimated temperatures are positive and negative due to underestimation and overestimation of stream water temperatures, respectively (Figure 5). Over the study period, estimated daily mean stream temperatures versus measured had an NSE of 0.64 (1 = good fit) and RMSE of 2.76°C (0 = good fit). The fit for maximum daily stream temperatures was poorer (NSE of 0.53; RMSE of 3.55°C) (Table 1, Figure 5). As the study period was characterised by highly variable conditions, we also analysed annual and seasonal periods. The NSEs were lowest during summer, when stream temperatures were usually underestimated, with negative NSEs and high CVs (Table 1). However, there were differences in goodness-of-fit between the drier summer of 2013 (lower saturation extents and, as such, less hydrological connectivity) and the wetter summer of 2014. In some winter periods (typically with reduced saturation extents), stream water temperatures were overestimated. Large events after or during dry conditions caused increased saturation extent, with sudden improvements in the estimated data fit for short periods, such as the large, transient increase in saturation extent in summer 2013. Overall, during periods of high saturation (i.e., high connectivity), the model fit was good for both maximum and mean daily temperatures (i.e., NSEs of 0.82 for mean and 0.78 for maximum temperatures in autumn 2013).

In the autumn and spring, the model fits depended on wetness. In autumn, there were generally very good predictions with high NSEs (Table 1). In contrast, spring was more variable; in the wet spring of 2013 NSEs were high with 0.72 (mean) and 0.75 (max), but lower (0.3 and –0.27 for mean and max temperature, respectively) in the drier spring of 2014 (Table 1). In short, the two end members adequately estimated stream water temperatures during wet conditions, but other factors influence stream water temperatures during dry conditions.

## Effect of saturation extent and atmospheric energy components on model performance

The correlations (Spearman's rank order) of the difference between measured and estimated temperatures for the daily mean and maximum temperatures with various energy balance components are given in Table 2. Results showed that there was no significant correlation with the saturated area extent for the whole period, although there were significant ($p < 0.05$) positive and negative correlations

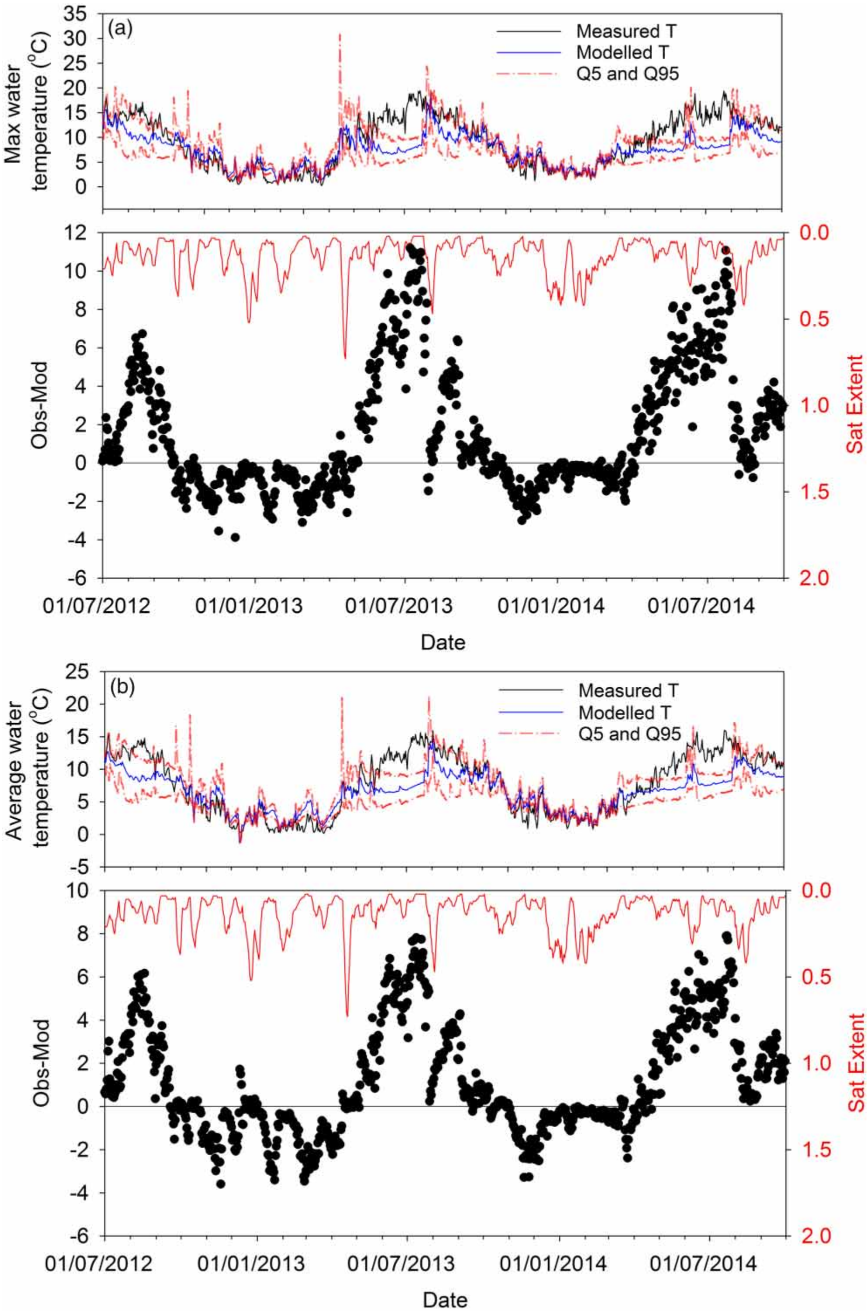


**Figure 5** | (a) Maximum temperature and (b) mean temperature. Time series of the measured versus simulated stream temperature, with stream temperatures estimated using the 95th and 5th percentiles (Q5 and Q95) of the modelled NSF and GW flow estimates. The lower plot shows the difference between measured and estimated temperature (measured minus the estimated), and catchment saturation extent as fraction of the catchment. 0 equals perfect data fit. Negative and positive values reflect an overestimation and underestimation of stream water temperatures, respectively.

for wet and dry periods, respectively (Table 2). For the entire study period, net radiation was most strongly correlated with the difference between measured minus estimated data, with poorest model fits in periods where net radiation was highest (e.g., summer 2013 and summer 2014). However, there was a significant ($p < 0.05$) negative correlation with GW levels, i.e., during wetter conditions and high water tables, data differences were lowest. Latent and sensible

**Table 1** | Performance measures for each of the data period

| | Mean temperature | | | | Max temperature | | | |
|---|---|---|---|---|---|---|---|---|
| **Period** | **NSE** | **KGE** | **RMSE (°C)** | **CV** | **NSE** | **KGE** | **RMSE (°C)** | **CV** |
| Full time series | 0.64 | 0.56 | 2.76 | 0.61 | 0.53 | 0.53 | 3.55 | 0.61 |
| Jul 12-Jul13 | 0.71 | 0.59 | 2.52 | 0.61 | 0.67 | 0.61 | 2.95 | 0.65 |
| Jul 13-Jul14 | 0.6 | 0.55 | 2.72 | 0.59 | 0.44 | 0.49 | 3.70 | 0.58 |
| Summer 12 | −8.18 | −0.05 | 3.48 | 1.12 | −5.55 | 0.14 | 3.51 | 1.32 |
| Autumn 12 | 0.76 | 0.65 | 1.46 | 0.66 | 0.71 | 0.63 | 1.70 | 0.66 |
| Winter 12-13 | −0.66 | 0.24 | 1.48 | 1.06 | −0.14 | 0.43 | 1.41 | 0.92 |
| Spring 13 | 0.72 | 0.55 | 1.88 | 0.55 | 0.75 | 0.66 | 2.20 | 0.68 |
| Summer 13 | −13.39 | 0.11 | 4.87 | 1.59 | −11.31 | −0.07 | 6.68 | 1.50 |
| Autumn 13 | 0.82 | 0.64 | 1.32 | 0.65 | 0.78 | 0.63 | 1.62 | 0.64 |
| Winter 13-14 | 0.58 | 0.76 | 0.82 | 1.09 | 0.68 | 0.81 | 0.78 | 1.08 |
| Spring 14 | 0.3 | 0.32 | 2.16 | 0.36 | −0.27 | 0.10 | 3.33 | 0.21 |
| Summer 14 | −9.08 | −0.17 | 4.41 | 1.03 | −8.52 | −0.28 | 5.75 | 1.15 |
| Autumn 14 | −6.37 | 0.35 | 2.27 | 0.44 | −7.64 | 0.59 | 2.83 | 0.79 |

NSE: Nash-Sutcliffe efficiency; KGE: Kling-Gupta efficiency; RMSE: root mean square error; CV: coefficient of variation.

**Table 2** | Correlation and significance of measured and estimated data differences versus saturation extent, GW level, net radiation, latent heat, and sensible heat for the full data period, a typical dry period (Summer 2013) and a typical wet period (Winter 2013–2014)

| Variable | Correlation |
|---|---|
| **Full period** | |
| Saturation extent | −0.04 |
| GW level | −0.56* |
| Net radiation | 0.72* |
| Latent heat | −0.42* |
| Sensible heat | −0.05 |
| **Summer dry period (June-September 2013)** | |
| Saturation extent | −0.64* |
| GW level | −0.39* |
| Net radiation | 0.58* |
| Latent heat | 0.11 |
| Sensible heat | −0.17 |
| **Winter wet period (December 2013 – March 2014)** | |
| Saturation extent | 0.62* |
| GW level | 0.44* |
| Net radiation | 0.04 |
| Latent heat | 0.03 |
| Sensible heat | 0.09 |

*Statistically significant.

heat fluxes had lower correlations and were only significant ($p < 0.05$) for the former.

During the dry summer of 2013, data differences were negatively correlated with the saturation area extent (r = −0.64). Likewise, lower correlations between the difference between measured and estimated temperatures and GW level were also negative and significant ($p < 0.05$), with a correlation coefficient of −0.39. Data differences were positively correlated with net radiation (r = 0.58; $p < 0.05$). Together with the negative correlation with saturation area extent, this would be consistent with greater importance of energy exchange at the atmosphere–stream interface, as the riparian area becomes disconnected during drier conditions.

In the wetter winter period 2013–14, predicted temperatures were best when the catchment was wettest, punctuated by periods of low saturation extent, lower connectivity and overprediction of stream water temperatures (Table 1 and Figure 5). Consequently, there were strong positive correlations (~0.62) between saturation extent and differences between measured and estimated data; with differences increasing as saturation extent decreased. Correlations were also positive between measured and estimated temperature differences and GW level during the winter (e.g., 0.44 in the winter of 2012–2014), suggesting that using the saturation extent was a good proxy for catchment wetness. There were no significant correlations with the energy balance components for the full winter periods.

## DISCUSSION

### Learning from model successes and failures

We used a simple mixing equation to increase our understanding of the role of NSFs and hydrological connectivity on stream temperatures. This is a relatively new approach in that few studies have investigated such linkages using temperature as a tracer (e.g., Shanley & Peters 1988), and even fewer have used temperature to infer processes through evaluating the implications of where such models are adequate and when they fail. A simple mixing equation is able to capture a surprisingly large amount of the variability in daily mean and maximum temperatures on the basis of mixing waters with the thermal properties of NSF and GW, particularly in wetter periods. However, energy exchange at the stream–atmosphere interface becomes more important when catchments are drier (McDonald & Urban 2010) and hydrological connectivity is reduced. This probably reflects additional energy inputs in summer when the saturated area is diminished in size, or conversely, long-wave energy losses in winter.

The data fit was best during the spring and winter, which correspond with prolonged periods of above-average catchment wetness and higher hydrological connectivity between the riparian wetland and the stream network (Soulsby *et al.* 2016). During these periods, the dominant control on stream water temperatures was simply the mixing of GW and NSF. However, similar good results were also evident in wet summer periods (Figure 5).

Periods with the poorest data fits coincided with drier periods where hydrological connectivity was reduced, and temperatures were underpredicted, most notably in summer. This probably reflects increased influence of incoming radiation at the stream–atmosphere interface, the lower saturated area and greatly reduced NSF (Smith & Lavis 1975; Sinokrot & Stefan 1994; Garner *et al.* 2015). Similar effects in winter likely reflect increased radiative losses from the stream–atmosphere interface, the lower thermal capacity of reduced flow volumes (van Vliet *et al.* 2011) and freezing of sources of NSF during cold, dry winter periods.

Maximum daily temperatures are a crucial metric for riverine systems, as they can regulate cold water species distributions (such as Atlantic salmon) through both lethal and sub-lethal effects (Garside 1973; Kurylyk *et al.* 2015). As with mean temperatures, the best performance was during periods of high wetness and hydrological connectivity. Over drier periods, the fit was substantially worse than that of mean temperatures, with the greater differences between measured and estimated temperatures. As with the underprediction of mean daily temperatures, the likely cause was the reduced NSFs as the riparian zone disconnected due to lowering of GW level and reduction in surface saturation. This led to a smaller surface area to volume ratio for atmospheric energy inputs to affect (Mohseni *et al.* 1999; Webb *et al.* 2003; van Vliet *et al.* 2011).

### Influence of riparian wetlands and hydrological connectivity on stream temperatures

We have highlighted the importance of the saturated area extent in riparian wetlands as a proxy for NSF contributions to streamflow and the resulting influence on stream temperatures. This was reflected in the close relationship between riparian GW levels and the extent of saturation, when the water table reaches the soil surface (i.e., when GW levels are high, saturation extent is also high) (Figure 3(g) and 3(h)), even though the GW response was more sensitive and dynamic than the saturation extent algorithm. Previous work at the site showed that high riparian GW levels indicate high connectivity with the stream network (Blumstock *et al.* 2015). Hence, there were similar patterns of correlations in the difference between measured and estimated temperatures and GW levels and saturation extent, with differences lowest when the water level was highest and the extent of riparian saturation was greatest (Table 2). During warmer periods in summer, when the saturation extent was reduced and connectivity limited, measured versus estimated fit was poor, due to increased influence of incoming radiation, which is a major component of energy budgets at the stream–atmosphere interface (Brown *et al.* 2010; Garner *et al.* 2015). In addition, reduced flows reduce the thermal capacity of the stream, increasing the influence of atmospheric energy exchanges on the smaller water volumes (Sinokrot & Gulliver 2000; Orr *et al.* 2015a, 2015b). In contrast, during wet conditions, the extent of the saturation area increases, which leads to greater connectivity between catchment and stream channel (Dick *et al.* 2014; Birkel *et al.* 2015; Mosquera *et al.* 2015). As the extent of saturation increases, so does the area contributing higher volumes of water to stream flow via NSF paths (Dick *et al.* 2014; Goulsbra *et al.* 2014). Abrupt improvements in data fit during transient wet periods, within the drier summer months, suggest that re-connection of the saturated riparian zones to the stream effectively re-sets the stream water temperature to that of the mixed GW and NSF. The fact that riparian peats are able to sustain high moisture contents, even in dry periods when fluxes to sustain stream flow decrease (Ingram 1983), would explain this rapid effect.

The saturated riparian wetland forms an area (a) where NSFs can be influenced by atmospheric energy exchanges over an extensive zone which can increase near-surface water temperatures, similar to findings of Callahan *et al.* (2015), (b) where mixing of these highly variable NSFs and more constant deeper GW can occur (Tetzlaff *et al.* 2014) and (c) where contributions of large and dominant volumes of NSFs to the stream channel network occur when connected. This connection is quasi-continuous, depending on antecedent conditions (Birkel *et al.* 2011). In drier periods, colder, deeper GW sources dominate (Tunaley *et al.* 2016). This suggests that in periods of high connectivity and high fluxes of NSF, stream temperatures are not influenced primarily by radiative inputs on the stream channel, but by inputs on the riparian wetlands.

Currently, there is increased interest in managing riparian zones to generate multiple benefits and maintain ecosystem services of aquatic ecosystems (Osborne & Kovacic 1993). Of particular attraction are 'buffer zones' fringing stream channels to concentrate management treatments in small, cost-effective areas (Castelle *et al.* 1994). In relation to stream temperature, buffer zones are areas where tree planting may be focused to reduce radiation inputs and moderate stream water temperatures (Correll 1996). Such techniques are usually prohibitively expensive to be extrapolated to entire catchments (Kuglerová *et al.* 2014), and there is much uncertainty around their effectiveness as a 'one size fits all' approach (Bowler *et al.* 2012). However, with climatic change, there is a need for land management that builds resilience and moderates stream temperatures (Orr *et al.* 2015a, 2015b). This raises questions over the optimal widths of buffer zones (Sweeney & Newbold 2014), with what are often site-specific requirements. Few studies have examined the influence of saturated riparian wetlands on stream temperatures and the implications these might have on temperature-orientated riparian management. Our study suggests stream thermal regimes may be at times influenced by areas considerably larger than narrow buffer strips, which may, in turn, limit their effectiveness. In such landscapes, more extensive riparian planting, with species tolerant of saturation, may need to be considered. This remains a fertile area for research.

Finally, such headwaters are important areas of the riverscape and impact ecosystem services downstream (Bishop *et al.* 2008). While this study specifically deals with water temperatures in a headwater catchment, they effect downstream waters indirectly, namely, their influence on biogeochemical processes (Alexander *et al.* 2007), their important biodiversity (Bishop *et al.* 2008) and the ability to dictate the distribution and survival of fauna (Hannah *et al.* 2004).

## CONCLUSION

We used a simple mixing equation to increase our understanding of how dynamic riparian wetlands, that often extend well beyond the channel network, can strongly influence stream water temperatures. These wetlands form important 'hot spots' of hydrological connectivity, where thermally variable near-surface waters mix with more stable deeper GW. The study has shown that a simple mixing model can explain stream water temperatures in terms of varying sources of these GW and near-surface sources during wetter conditions, in both winter and summer. This was consistent with energy exchanges between the saturated area and atmosphere dominating the processes affecting stream temperatures. In drier conditions, where the area of saturation was reduced, energy exchanges at the stream–atmosphere interface became more important, and high net radiation raises water temperatures in the channel network. During winter low flows and low connectivity periods, long-wave losses occur. GW also has a contrasting role in summer and winter giving a cooling effect in the former but a significant heat source in the latter. The identification of extended riparian areas, as important components in the system that govern stream temperatures, has implications for riparian management strategies that target the stream bank for planting schemes. These were aimed at reducing stream temperatures and building ecosystem resilience to climate warming. Larger areas may be needed for planting where riparian zones are characterised by extensive wetlands.

## ACKNOWLEDGEMENTS

We would like to thank the Leverhulme Trust (project PLATO, RPG-2014-016) for funding. We also thank two anonymous reviewers for their invaluable comments that improved the manuscript.

## REFERENCES

Ala-aho, P., Soulsby, C., Wang, H. & Tetzlaff, D. 2017 Integrated surface-subsurface model to investigate the role of groundwater in headwater catchment runoff generation: a minimalist approach to parameterisation. *Journal of Hydrology* **547**, 664–677.

Alexander, R. B., Boyer, E. W., Smith, R. A., Schwarz, G. E. & Moore, R. B. 2007 The role of headwater streams in downstream water quality. *Journal of the American Water Resources Association* **43** (1), 41–59. doi:10.1111/j.1752-1688.2007.00005.x.

Birkel, C., Tetzlaff, D., Dunn, S. M. & Soulsby, C. 2010 Towards a simple dynamic process conceptualization in rainfall–runoff models using multi-criteria calibration and tracers in temperate, upland catchments. *Hydrological Processes* **24** (3), 260–275. doi:10.1002/hyp.7478.

Birkel, C., Soulsby, C. & Tetzlaff, D. 2011 Modelling catchment-scale water storage dynamics: reconciling dynamic storage with tracer-inferred passive storage. *Hydrological Processes* **25** (25), 3924–3936. doi:10.1002/hyp.8201.

Birkel, C., Soulsby, C. & Tetzlaff, D. 2015 Conceptual modelling to assess how the interplay of hydrological connectivity, catchment storage and tracer dynamics controls nonstationary water age estimates. *Hydrological Processes* **29** (13), 2956–2969. doi:10.1002/hyp.10414.

Birkel, C., Soulsby, C., Irvine, D. J., Malcolm, I., Lautz, L. K. & Tetzlaff, D. 2016 Heat-based hyporheic flux calculations in heterogeneous salmon spawning gravels. *Aquatic Sciences* **78** (2), 203–13. https://doi.org/10.1007/s00027-015-0417-4.

Bishop, K., Buffam, I., Erlandsson, M., Fölster, J., Laudon, H., Seibert, J. & Temnerud, J. 2008 Aqua incognita: the unknown headwaters. *Hydrological Processes* **22** (8), 1239–1242.

Blumstock, M., Tetzlaff, D., Malcolm, I. A., Nuetzmann, G. & Soulsby, C. 2015 Baseflow dynamics: multi-tracer surveys to assess variable groundwater contributions to montane streams under low flows. *Journal of Hydrology* **527**, 1021–1033. doi:10.1016/j.jhydrol.2015.05.019.

Bowler, D. E., Mant, R., Orr, H., Hannah, D. M. & Pullin, A. S. 2012 What are the effects of wooded riparian zones on stream temperature? *Environmental Evidence* **1** (1), 3. doi:10.1186/2047-2382-1-3.

Broadmeadow, S. B., Jones, J. G., Langford, T. E. L., Shaw, P. J. & Nisbet, T. R. 2011 The influence of riparian shade on lowland stream water temperatures in southern England and their viability for brown trout. *River Research and Applications* **27** (2), 226–237.

Brown, L. E., Cooper, L., Holden, J. & Ramchunder, S. J. 2010 A comparison of stream water temperature regimes from open and afforested moorland, Yorkshire Dales, northern England. *Hydrological Processes* **24** (22), 3206–3218.

Buttle, J. M. 1994 Isotope hydrograph separations and rapid delivery of pre-event water from drainage basins. *Progress in Physical Geography* **18** (1), 16–41. doi:10.1177/030913339401800102.

Caissie, D. 2006 The thermal regime of rivers: a review. *Freshwater Biology* **51** (8), 1389–1406. doi:10.1111/j.1365-2427.2006.01597.x.

Callahan, M. K., Rains, M. C., Bellino, J. C., Walker, C. M., Baird, S. J., Whigham, D. F. & King, R. S. 2015 Controls on temperature in salmonid-bearing headwater streams in two common hydrogeologic settings, Kenai Peninsula, Alaska. *Journal of the American Water Resources Association* **51** (1), 84–98. doi:10.1111/jawr.12235.

Castelle, A. J., Johnson, A. W. & Conolly, C. 1994 Wetland and stream buffer size requirements – a review. *Journal of Environment Quality* **23** (5), 878. doi:10.2134/jeq1994.00472425002300050004x.

Constantz, J. 1998 Interaction between stream temperature, streamflow, and groundwater exchanges in alpine streams. *Water Resources Research* **34** (7), 1609–1615. doi:10.1029/98WR00998.

Correll, D. L. 1996 Buffer zones and water quality protection: General principles. In: *Buffer Zones: Their Processes and Potential in Water Protection. The Proceedings of the International Conference on Buffer Zones*, pp. 7–20. http://biodiversitysouthwest.org.uk/docs/BufferZones(locked).pdf#page=15.

Dick, J. J., Tetzlaff, D., Birkel, C. & Soulsby, C. 2014 Modelling landscape controls on dissolved organic carbon sources and fluxes to streams. *Biogeochemistry* **2–3**, 361–374.

Dick, J. J., Tetzlaff, D. & Soulsby, C. 2015 Landscape influence on small-scale water temperature variations in a moorland catchment. *Hydrological Processes* **29** (14), 3098–3111. doi:10.1002/hyp.10423.

Dunne, T., Moore, T. R. & Taylor, C. H. 1975 Recognition and prediction of runoff-producing zones in humid regions. *Hydrological Science–Bulletin–des Sciences Hydrologiques*. http://agris.fao.org/agris-search/search.do?recordID=US201303050196.

Garner, G., Malcolm, I. A., Sadler, J. P., Millar, C. P. & Hannah, D. M. 2015 Inter-annual variability in the effects of riparian woodland on micro-climate, energy exchanges and water temperature of an upland Scottish stream. *Hydrological Processes* **29** (6), 1080–1095. doi:10.1002/hyp.10223.

Garside, E. T. 1973 Ultimate upper lethal temperature of Atlantic salmon *Salmo Salar* L. *Canadian Journal of Zoology* **51** (8), 898–900. doi:10.1139/z73-135.

Geris, J., Tetzlaff, D., McDonnell, J. & Soulsby, C. 2014 The relative role of soil type and tree cover on water storage and transmission in northern headwater catchments. *Hydrological Processes*. http://onlinelibrary.wiley.com/doi/10.1002/hyp.10289/full.

Goulsbra, C., Evans, M. & Lindsay, J. 2014 Temporary streams in a peatland catchment: pattern, timing, and controls on stream network expansion and contraction. *Earth Surface Processes and Landforms* **39** (6), 790–803. doi:10.1002/esp.3533.

Gupta, H. V., Kling, H., Yilmaz, K. K. & Martinez, G. F. 2009 Decomposition of the mean squared error and NSE performance criteria: implications for improving hydrological modelling. *Journal of Hydrology* **377** (1–2), 80–91. doi:10.1016/j.jhydrol.2009.08.003.

Hannah, D. M., Malcolm, I. A., Soulsby, C. & Youngson, A. F. 2004 Heat exchanges and temperatures within a salmon spawning stream in the Cairngorms, Scotland: seasonal and sub-seasonal dynamics. *River Research and Applications* **20** (6), 635–652.

Hrachowitz, M., Soulsby, C., Imholt, C., Malcolm, I. A. & Tetzlaff, D. 2010 Thermal regimes in a large upland salmon river: a simple model to identify the influence of landscape controls and climate change on maximum temperatures. *Hydrological Processes* **24** (23), 3374–3391. doi:10.1002/hyp.7756.

Imholt, C., Soulsby, C., Malcolm, I. A., Hrachowitz, M., Gibbins, C. N., Langan, S. & Tetzlaff, D. 2013 Influence of scale on thermal characteristics in a large montane river basin. *River Research and Applications* **29** (4), 403–419. doi:10.1002/rra.1608.

Ingram, H. A. P. 1983 Hydrology. In: *Mires: Swamp, Bog, Fen and Moor* (A. J. P. Gore, ed.). Elsevier, Oxford, pp. 67–158.

Isaak, D. J. & Hubert, W. A. 2001 A hypothesis about factors that affect maximum summer stream temperatures across montane landscapes. *Journal of the American Water Resources Association* **37**, 351–366.

Johnson, M. F. & Wilby, R. L. 2015 Seeing the landscape for the trees: metrics to guide riparian shade management in river catchments. *Water Resources Research* **51** (5), 3754–3769. doi:10.1002/2014WR016802.

Kendall, C. & McDonnell, J. J. 1998 *Isotope Tracers in Catchment Hydrology*. Elsevier, Amsterdam.

Kuglerová, L., Ågren, A., Jansson, R. & Laudon, H. 2014 Towards optimizing riparian buffer zones: ecological and biogeochemical implications for forest management. *Forest Ecology and Management* **334**, 74–84. doi:10.1016/j.foreco.2014.08.033.

Kurylyk, B. L., MacQuarrie, K. T. B. & Voss, C. I. 2014 Climate change impacts on the temperature and magnitude of groundwater discharge from shallow, unconfined aquifers. *Water Resources Research* **50** (4), 3253–3274. doi:10.1002/2013WR014588.

Kurylyk, B. L., MacQuarrie, K. T. B., Linnansaari, T., Cunjak, R. A. & Curry, R. A. 2015 Preserving, augmenting, and creating cold-water thermal refugia in rivers: concepts derived from research on the Miramichi River, New Brunswick (Canada). *Ecohydrology* **8** (6), 1095–1108. doi:10.1002/eco.1566.

Malcolm, I. A., Hannah, D. M., Donaghy, M. J., Soulsby, C. & Youngson, A. F. 2004 The influence of riparian woodland on the spatial and temporal variability of stream water temperatures in an upland salmon stream. *Hydrology and Earth System Sciences* **8** (3), 449–59. https://doi.org/10.5194/hess-8-449-2004.

McDonald, C. P. & Urban, N. R. 2010 Using a model selection criterion to identify appropriate complexity in aquatic biogeochemical models. *Ecological Modelling* **221** (3), 428–432. doi:10.1016/j.ecolmodel.2009.10.021.

McNamara, J. P., Kane, D. L. & Hinzman, L. D. 1997 Hydrograph separations in an Arctic watershed using mixing model and graphical techniques. *Water Resources Research* **33** (7), 1707–1719. doi:10.1029/97WR01033.

Met Office 2012 Summer 2012. Reference. Met Office. December 11. http://www.metoffice.gov.uk/climate/uk/summaries/2012/summer.

Met Office 2013a Winter 2012/13. Reference. Met Office. February 11. http://www.metoffice.gov.uk/climate/uk/summaries/2013/winter.

Met Office 2013b Spring 2013. Reference. Met Office. March 7. http://www.metoffice.gov.uk/climate/uk/summaries/2013/spring.

Met Office 2013c Summer 2013. Reference. Met Office. March 26. http://www.metoffice.gov.uk/climate/uk/summaries/2013/summer.

Met Office 2014 Winter 2014. Reference. Met Office. March 26. http://www.metoffice.gov.uk/climate/uk/summaries/2014/winter.

Mohseni, O., Erickson, T. R. & Stefan, H. G. 1999 Sensitivity of stream temperatures in the United States to air temperatures projected under a global warming scenario. *Water Resources Research* **35** (12), 3723–3733. doi:10.1029/1999WR900193.

Mosley, M. P. 1983 Variability of water temperatures in the Braided Ashley and Rakaia Rivers. *New Zealand Journal of Marine and Freshwater Research* **17** (3), 331–342. doi:10.1080/00288330.1983.9516007.

Mosquera, G. M., Lazo, P. X., Célleri, R., Wilcox, B. P. & Crespo, P. 2015 Runoff from tropical alpine grasslands increases with areal extent of wetlands. *CATENA* **125**, 120–128. doi:10.1016/j.catena.2014.10.010.

Murphy, J. M., Sexton, D. M. H., Jenkins, G. J., Boorman, P. M., Booth, B. B. B., Brown, C. C., Clark, R. T., Collins, M., Harris, G. & Kendon, L. 2009 *UK Climate Projections Science Report: UKCP09*. Met Office Hadley Centre, Exeter, UK.

Nash, J. E. & Sutcliffe, J. V. 1970 River flow forecasting through conceptual models part I – a discussion of principles. *Journal of Hydrology* **10** (3), 282–290. doi:10.1016/0022-1694(70)90255-6.

Ockenden, M. C., Chappell, N. A. & Neal, C. 2014 Quantifying the differential contributions of deep groundwater to streamflow in nested basins, using both water quality characteristics and water balance. *Hydrology Research* **45** (2), 200–212. doi:10.2166/nh.2013.035.

Orr, H. G., Johnson, M. F., Wilby, R. L., Hatton-Ellis, T. & Broadmeadow, S. 2015a What else do managers need to know about warming rivers? A United Kingdom perspective: managing warming rivers. *Wiley Interdisciplinary Reviews: Water* **2** (2), 55–64. doi:10.1002/wat2.1062.

Orr, H. G., Simpson, G. L., des Clers, S., Watts, G., Hughes, M., Hannaford, J., Dunbar, M. J., Laize, C. L. R., Wilby, R. L., Battarbee, R. W. & Evans, R. 2015b Detecting changing river temperatures in England and Wales. *Hydrological Processes* **29** (5), 752–766. doi:10.1002/hyp.10181.

Osborne, L. L. & Kovacic, D. A. 1993 Riparian vegetated buffer strips in water-quality restoration and stream management. *Freshwater Biology* **29** (2), 243–258. doi:10.1111/j.1365-2427.1993.tb00761.x.

Scheliga, B., Tetzlaff, D. & Soulsby, C. 2017 Groundwater isoscapes in a montane headwater catchment show dominance of time invariant well-mixed sources. *Hydrological Processes*. **31** (20), 3504–3519. doi:10.1002/hyp.11271

Selker, J., van de Giesen, N., Westhoff, M., Luxemburg, W. & Parlange, M. B. 2006 Fiber optics opens window on stream dynamics. *Geophysical Research Letters* **33**. doi:200610.1029/2006GL027979.

Shanley, J. B. & Peters, N. E. 1988 Preliminary observations of streamflow generation during storms in a forested piedmont watershed using temperature as a tracer. *Journal of Contaminant Hydrology* **3** (2–4), 349–365. doi:10.1016/0169-7722(88)90040-X.

Sinokrot, B. A. & Gulliver, J. S. 2000 In-stream flow impact on river water temperatures. *Journal of Hydraulic Research* **38** (5), 339–349. doi:10.1080/00221680009498315.

Sinokrot, B. A. & Stefan, H. G. 1994 Stream water-temperature sensitivity to weather and bed parameters. *Journal of Hydraulic Engineering* **120** (6), 722–736. doi:10.1061/(ASCE)0733-9429(1994)120:6(722).

Smith, K. & Lavis, M. E. 1975 Environmental influences on the temperature of a small upland stream. *Oikos* **26** (2), 228–236. doi:10.2307/3543713.

Soulsby, C., Birkel, C., Geris, J., Dick, J., Tunaley, C. & Tetzlaff, D. 2015 Stream water age distributions controlled by storage dynamics and nonlinear hydrologic connectivity: modeling with high-resolution isotope data. *Water Resources Research* **51** (9), 7759–7776. doi:10.1002/2015WR017888.

Soulsby, C., Birkel, C. & Tetzlaff, D. 2016 Modelling storage-driven connectivity between landscapes and riverscapes: towards a simple framework for long-term ecohydrological assessment. *Hydrological Processes* **30** (14), 2482–2497.

Sweeney, B. W. & Newbold, J. D. 2014 Streamside forest buffer width needed to protect stream water quality, habitat, and organisms: a literature review. *Journal of the American Water Resources Association* **50** (3), 560–584. doi:10.1111/jawr.12203.

Tetzlaff, D., Soulsby, C., Waldron, S., Malcolm, I. A., Bacon, P. J., Dunn, S. M., Lilly, A. & Youngson, A. F. 2007 Conceptualization of runoff processes using a geographical information system and tracers in a nested mesoscale catchment. *Hydrological Processes* **21** (10), 1289–1307.

Tetzlaff, D., Birkel, C., Dick, J., Geris, J. & Soulsby, C. 2014 Storage dynamics in hydropedological units control hillslope connectivity, runoff generation, and the evolution of catchment transit time distributions. *Water Resources Research* **50** (2), 969–985. doi:10.1002/2013WR014147.

Tunaley, C., Tetzlaff, D., Lessels, J. & Soulsby, C. 2016 Linking high-frequency DOC dynamics to the age of connected water sources. *Water Resources Research* **52** (7), 5232–5247.

van Vliet, M. T. H., Ludwig, F., Zwolsman, J. J. G., Weedon, G. P. & Kabat, P. 2011 Global river temperatures and sensitivity to atmospheric warming and changes in river flow. *Water Resources Research* **47** (2). doi:10.1029/2010WR009198.

Webb, B. W., Clack, P. D. & Walling, D. E. 2003 Water–air temperature relationships in a Devon river system and the role of flow. *Hydrological Processes* **17** (15), 3069–3084. doi:10.1002/hyp.1280.

Zwieniecki, M. A. & Newton, M. 1999 Influence of streamside cover and stream features on temperature trends in forested streams of Western Oregon. *Western Journal of Applied Forestry* **14** (2), 106–113.

First received 5 April 2017; accepted in revised form 23 September 2017. Available online 13 November 2017